



Apparent diffusion coefficient mapping using diffusion-weighted MRI: impact of background parenchymal enhancement, amount of fibroglandular tissue and menopausal status on breast cancer diagnosis

Joao V. Horvat¹ · Manuela Durando^{1,2} · Soledad Milans^{1,3} · Sujata Patil⁴ · Jessica Massler^{1,5} · Girard Gibbons¹ · Dilip Giri⁶ · Katja Pinker^{1,7} · Elizabeth A. Morris¹ · Sunitha B. Thakur^{1,8}

Received: 9 September 2017 / Revised: 14 November 2017 / Accepted: 22 November 2017
© European Society of Radiology 2018

Abstract

Objectives To investigate the impact of background parenchymal enhancement (BPE), amount of fibroglandular tissue (FGT) and menopausal status on apparent diffusion coefficient (ADC) values in differentiation between malignant and benign lesions.

Methods In this HIPAA-compliant study, mean ADC values of 218 malignant and 130 benign lesions from 288 patients were retrospectively evaluated. The differences in mean ADC values between benign and malignant lesions were calculated within groups stratified by BPE level (high/low), amount of FGT (dense/non-dense) and menopausal status (premenopausal/postmenopausal). Sensitivities and specificities for distinguishing malignant from benign lesions within different groups were compared for statistical significance.

Results The mean ADC value for malignant lesions was significantly lower compared to that for benign lesions ($1.07 \pm 0.21 \times 10^{-3} \text{ mm}^2/\text{s}$ vs. $1.53 \pm 0.26 \times 10^{-3} \text{ mm}^2/\text{s}$) ($p < 0.0001$). Using the optimal cut-off point of $1.30 \times 10^{-3} \text{ mm}^2/\text{s}$, an area under the curve of 0.918 was obtained, with sensitivity and specificity both of 87 %. There was no statistically significant difference in sensitivities and specificities of ADC values between different groups stratified by BPE level, amount of FGT or menopausal status.

Conclusions Differentiation between benign and malignant lesions on ADC values is not significantly affected by BPE level, amount of FGT or menopausal status.

Joao V. Horvat and Manuela Durando contributed equally to this work.

✉ Sunitha B. Thakur
thakurs@mskcc.org

¹ Department of Radiology, Breast Imaging Service, Memorial Sloan Kettering Cancer Center, New York, NY, USA

² Department of Diagnostic Imaging and Radiotherapy, A. O. U. Città della Salute e della Scienza di Torino, Turin, Italy

³ Hospital de Clínicas, University of the Republic, Montevideo, Uruguay

⁴ Department of Biostatistics, Memorial Sloan Kettering Cancer Center, New York, NY, USA

⁵ Department of Surgery, Memorial Sloan Kettering Cancer Center, New York, NY, USA

⁶ Department of Pathology, Memorial Sloan Kettering Cancer Center, New York, NY, USA

⁷ Department of Biomedical Imaging and Image-guided Therapy, Division of Molecular and Gender Imaging, Medical University of Vienna, Vienna, Austria

⁸ Department of Medical Physics, Memorial Sloan Kettering Cancer Center, 00 East 66th Street, New York, NY 10065, USA

Key Points

- ADC allows differentiation between benign and malignant lesions.
- ADC is useful for breast cancer diagnosis despite different patient characteristics.
- BPE, FGT or menopause do not significantly affect sensitivity and specificity.

Keywords Breast neoplasms · Diffusion magnetic resonance imaging · Diagnostic imaging · Breast density · Menopause

Abbreviations

ADC	Apparent diffusion coefficient
AUC	Area under the curve
BIRADS	Breast Imaging Reporting and Data System
BPE	Background parenchymal enhancement
DWI	Diffusion-weighted imaging
DCE	Dynamic contrast-enhancement
FGT	Fibroglandular tissue
MRI	Magnetic resonance imaging
ROC	Receiving operator characteristic
SD	Standard deviation

Introduction

Magnetic resonance imaging (MRI) is a quintessential tool for breast cancer diagnosis. Due to its high sensitivity, it has several established clinical indications including pre-operative staging, evaluation of treatment response in patients receiving neoadjuvant therapy, differentiation between scar tissue and tumour recurrence, examination of patients with breast implants, and screening of high-risk patients [1, 2]. Currently, dynamic contrast-enhanced MRI (DCE-MRI) is the most sensitive test for the diagnosis of breast cancer with good specificity [3–5]. Moreover, in the past few decades, efforts have been made to further improve the diagnostic accuracy of DCE-MRI [6], with several functional MRI parameters having been investigated for their utility in improving the diagnostic accuracy of DCE-MRI [7, 8]. Diffusion-weighted imaging (DWI) has emerged as the most reliable MRI parameter for an improved diagnosis and characterization of breast cancer in a multiparametric setting [9, 10].

DWI is a non-contrast MRI technique, sensitive to the random motion of water molecules in tissues [11]. Water diffusivity can be quantified using the apparent diffusion coefficient (ADC), which varies according to the amount of cellularity, intracellular and extracellular oedema, viscosity and fibrosis [12–14]. Numerous studies have evaluated DWI with ADC mapping for the diagnosis of breast tumours. It has been shown that ADC as a quantitative imaging biomarker can be used to differentiate malignant from benign lesions with high sensitivity and specificity of up to 98 % and 93 %, respectively [9, 10, 15–19].

Although DWI with ADC mapping is being implemented in clinical routine care, it is still unclear which patient characteristics may affect ADC values and what their impact is on the diagnostic accuracy of DWI. A few preliminary reports have addressed the impact of different patient characteristics, including background parenchymal enhancement (BPE), amount of fibroglandular tissue (FGT) and menopausal status on ADC values but with conflicting results [20–28]. In addition, it has also been reported that breast tissue composition can influence intravoxel signals of breast tumours and alter their ADC values [29]. To date, however, there are no data on whether BPE, FGT and menopausal status can affect the diagnostic accuracy of ADC for breast cancer detection.

Therefore, the goal of the study was to investigate the impact of BPE, FGT and menopausal status on ADC measurements and cancer diagnosis in patients with breast tumours.

Materials and methods

This single-institution retrospective study was compliant with Health Insurance Portability and Accountability Act

guidelines and approved by the Institutional Review Board with a waiver of informed consent.

Patient selection

We queried our institutional database for all consecutive patients who underwent multiparametric 3.0T MRI of the breast combining T2-weighted, DCE-MRI and DWI imaging between January 2011 and January 2013. The search yielded 854 results. We then applied the following exclusion criteria: (1) Breast Imaging Reporting and Data System (BI-RADS®) 0–3 classification on the MRI report; (2) treatment received prior to MRI examination; (3) histopathological verification of suspicious imaging findings by either image-guided or surgical biopsy unavailable; (4) lesions measuring less than 0.8 cm on contrast-enhanced T1-weighted sequence; and (5) DWI images hampered by artifacts or suboptimal fat suppression. Thus, a total of 288 patients were included in our study.

MRI acquisition

MR imaging was performed on a 3.0T system (Discovery MR750; GE Healthcare, WI, USA) using the body coil as a transmitter and a dedicated 16-channel phased-array receiver coil (Sentinelle Vanguard, Toronto, Canada). Conventional T1-weighted (3D T1-weighted gradient echo VIBRANT sequence; TR/TE 4.3/2.1 ms; flip angle 10°; matrix size 320x192; field of view (FOV) 30 cm; slice thickness 1 mm; number of excitations (NEX) 1; acquisition time ~1 min) as well as T2-weighted (fast spin-echo sequence with TR/TE 4,384/102 ms; auto flip angle 111°; matrix size 288x224; FOV 30 cm; slice thickness 3 mm; NEX 2; acquisition time ~3.5 min) images were acquired with and without fat suppression.

Axial DWI MR imaging was performed using 2D, DW single-shot, dual spin echo-planar imaging (EPI) sequences (TR 6,000 ms; minimum TE; flip angle 90°; acquisition matrix: 98x98 or 128x128; reconstructed matrix: 256x256; FOV 28–38 cm; slice thickness: 4 or 5 mm; NEX 3; slice gap: 0–1 mm; fat suppression: enhanced; parallel imaging: ASSET; acquisition time ~2 min for 2 b-values). In all the patients, DWI was acquired at b-values of 0 and 600 s/mm².

DCE-MRI images were acquired using a sagittal 3D T1-weighted sequence before and at three points at 60-s intervals after an injection of 0.1 mmol/kg of gadopentetate dimeglumine (Magnevist; Bayer HealthCare, Hanover, NJ, USA). Subsequently, axial 3D T1-weighted gradient echo VIBRANT delayed contrast-enhanced imaging was performed.

Data and image evaluation

All MRI studies and patient medical records were reviewed by a single dedicated breast radiologist (M.D.) who had 7 years of experience in breast MRI. The radiologist had access to patient data, including age, menopausal status and imaging study reports, but was blinded to pathological data. Menopausal status was classified into premenopausal and postmenopausal, defined as at least 1 year of amenorrhoea. The information acquired was annotated and compiled using a standardized form.

MRI

Images were analysed on a GE Advantage Workstation (GE Healthcare). Lesions were identified on MRI using DCE-MRI images and the longest transverse axis was measured as the lesion size. BPE was assessed on the first post-contrast sequence and the amount of FGT was assessed on T1 images without fat saturation. Both BPE and FGT classifications were performed according to the 5th edition BI-RADS [30]. BPE was classified as minimal, mild, moderate or marked. The amount of FGT was classified as almost entirely fat, scattered, heterogeneous or extreme FGT. When there was asymmetry of BPE or amount of FGT, the breast with the largest lesion was considered the reference standard.

DWI

The slice location with the largest transverse axis on T1-weighted DCE-MRI was used to identify the closest image

location of the lesion on DWI. High b-value DWI images were visually assessed for hyperintensities matched to enhancing lesions on DCE-MRI. Subsequently, parametric quantitative ADC maps were generated using READY View software (GE Healthcare). Mean ADC values were calculated by manually selecting a 2D region of interest covering most parts of the lesion, but avoiding cystic or necrotic portions, surrounding normal tissue and susceptibility artifacts due to the presence of post-biopsy clips or changes.

Histopathological analysis

In all patients, histopathology was used as the standard of reference. Histopathological reports of the breast lesions were reviewed and breast lesions were classified as either malignant or benign, which included high-risk lesions. Histopathology from surgical specimens was considered the reference

Table 1 Patient characteristics

Characteristics of patients	N	%
Patient age		
Mean 49 years \pm 10 SD (range, 23–81)		
Amount of fibroglandular tissue ^a		
Non-dense breast	53	18.4
Dense breast	235	81.6
Background parenchymal enhancement ^b		
Low BPE	145	50.3
High BPE	143	49.7
Menopausal status		
Premenopausal	158	54.9
Postmenopausal	130	45.1
Total number of patients	288	100

BPE background parenchymal enhancement, SD standard deviation

^a Non-dense was defined as fatty and scattered amount of fibroglandular tissue and dense as heterogeneous and extreme

^b Low BPE includes minimal and mild BPE and high includes moderate and marked

Table 2 Characteristics of lesions

Characteristics of lesions	N	%
Malignant lesions		
Number of lesions	218	62.6
Mean size (range), cm	2.8 (0.8–12)	
Histopathological type		
Invasive ductal carcinoma	148	42.5
Invasive lobular carcinoma	27	7.8
Ductal carcinoma <i>in situ</i>	35	10.1
Ductal carcinoma <i>in situ</i> with microinvasion	3	0.8
Other	5	1.4
Benign lesions		
Number of lesions	130	37.4
Mean size (range), cm	1.8 (0.8–8)	
Histopathological type		
High risk lesions	23	6.6
Papilloma	8	2.3
Lobular carcinoma <i>in situ</i>	5	1.4
Atypical lobular hyperplasia	5	1.4
Atypical ductal hyperplasia	4	1.2
Radial scar	1	0.3
Other benign lesions	107	30.8
Dense stromal fibrosis	20	5.8
Fibroadenoma	17	4.9
Pseudoangiomatous stromal hyperplasia	14	4.0
Fat necrosis	8	2.3
Sclerosing adenosis	8	2.3
Fibrocystic changes	8	2.3
Usual ductal hyperplasia	7	2.0
Other	25	7.2
Total number of lesions	348	100

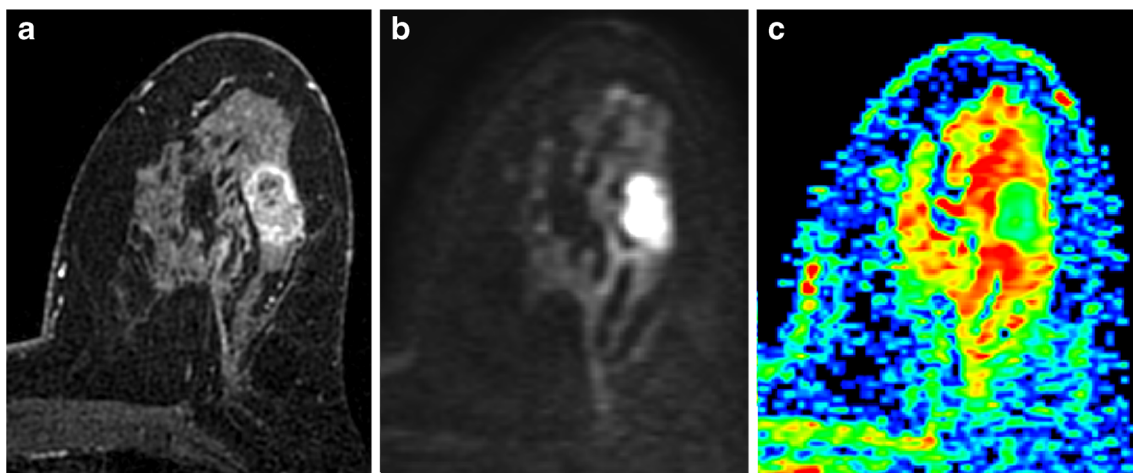


Fig. 1 A 49-year-old postmenopausal woman with dense breasts and low background parenchymal enhancement. In the left breast, an irregular mass with rim enhancement is noted on T1-weighted contrast enhanced

(a), diffusion-weighted imaging (DWI) (b) and ADC map (c) images. The mean ADC value obtained was $0.949 \times 10^{-3} \text{ mm}^2/\text{s}$. Biopsy yielded invasive ductal carcinoma

standard, and when it was not available, histopathology from breast biopsy samples were used.

Statistical analysis

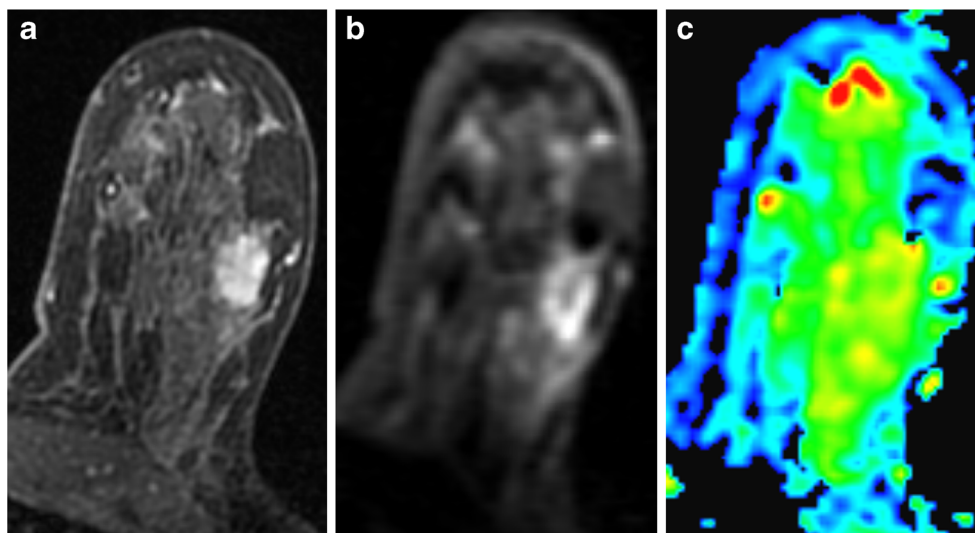
For statistical analysis, BPE and FGT classifications were dichotomized. Breasts with minimal or mild BPE were considered as ‘low’ BPE and breasts with moderate or marked BPE were considered as ‘high’ BPE. Breasts with almost entirely fat or scattered FGT composition were considered as ‘non-dense’ and breasts with heterogeneous or extreme FGT composition were considered as ‘dense’.

ADC values were presented as mean \pm standard deviation (SD) measured in units of $10^{-3} \text{ mm}^2/\text{s}$. ADC values were measured on a ‘lesion-by-lesion’ basis and bilateral lesions

in the same patient were assumed to be non-correlated. All ADC values were examined for normality and comparisons were made using two-sample t-tests or non-parametric tests as necessary. The overall sensitivity and specificity of ADC for identifying malignant lesions was plotted using a receiver operating characteristic (ROC) curve and the optimal cut-off point for ADC was identified using Youden’s index [31]. To determine the impact of BPE, FGT and menopausal status on ADC sensitivity and specificity, we used this cut-off point in a chi-square test to compare groups of patients stratified according to the respective dichotomized categories.

All statistical tests were two-tailed and the significance was established at $p < 0.05$. The analysis for this study was generated using SAS v9.4 software (SAS Institute Inc., Cary, NC, USA).

Fig. 2 A 39-year-old premenopausal woman with dense breasts and low background parenchymal enhancement. In the left breast, a 1.7 cm heterogeneously enhancing mass with circumscribed margins is noted on T1-weighted contrast enhanced (a), diffusion-weighted imaging (DWI) (b) and ADC map (c) images. The mean ADC value obtained was $1.670 \times 10^{-3} \text{ mm}^2/\text{s}$. Biopsy yielded fibroadenoma



Results

A total of 348 lesions in 288 women were identified. The mean patient age was 49 years (range, 23–81 years). There were 218 malignant and 130 benign lesions, including 23 high-risk and 107 other benign lesions, with a mean size of 2.4 cm (range 0.8–12 cm). The patient characteristics are demonstrated in Table 1 and the characteristics of the lesions are summarized in Table 2.

The mean ADC (\pm SD) value for malignant lesions was lower compared to that for benign lesions ($1.07 \pm 0.21 \times 10^{-3} \text{ mm}^2/\text{s}$ vs. $1.53 \pm 0.26 \times 10^{-3} \text{ mm}^2/\text{s}$), with a statistically significant difference ($p < 0.0001$). Representative images of DCE-MRI, DWI and ADC mapping images for malignant and benign lesions are demonstrated by Figs. 1 and 2. ROC curve analysis yielded an optimal ADC cut-off value of $1.30 \times 10^{-3} \text{ mm}^2/\text{s}$ with an area under the curve (AUC) of 0.918 (Fig. 3).

The overall and stratified ADC sensitivities and specificities are summarized in Table 3. There were no statistically significant differences in sensitivity and specificity for ADC in differentiating malignant and benign lesions in groups of patients separated by BPE level, amount of FGT or menopausal status.

Table 4 summarizes the mean ADC values for benign and malignant breast lesions stratified by BPE, FGT and menopausal status. When patients were stratified as low and high BPE, there was a significant difference in the ADC values of

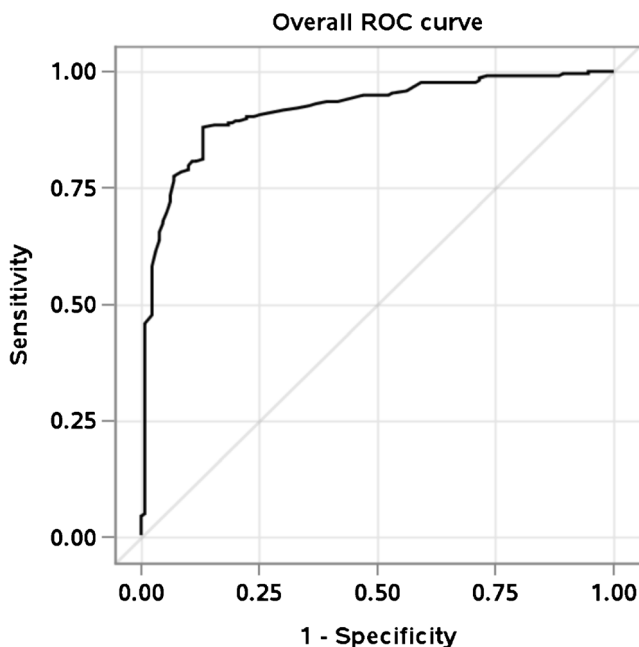


Fig. 3 Receiver operator characteristic (ROC) curve analysis of ADC values from overall breast lesions for differentiation between benign and malignant lesions

Table 3 Comparison of sensitivities and specificities in groups according to background parenchymal enhancement (BPE), amount of fibroglandular tissue (FGT) and menopausal status using the ADC cut-off value of $1.30 \times 10^{-3} \text{ mm}^2/\text{s}$

Variable	Sensitivity	<i>p</i> -value*	Specificity	<i>p</i> -value**
Overall lesions	87 %		87 %	
Background parenchymal enhancement				
Low BPE	83 %	0.0675	86 %	0.7948
High BPE	91 %		88 %	
Amount of fibroglandular tissue				
Non-dense	87 %	0.9856	75 %	0.0856
Dense	87 %		89 %	
Menopausal status				
Premenopausal	89 %	0.4310	90 %	0.2610
Postmenopausal	85 %		83 %	

ADC apparent diffusion coefficient, BPE background parenchymal enhancement, FGT fibroglandular tissue

*Of comparison between sensitivities in the different groups

**Of comparison between specificities in the different groups

benign and malignant lesions ($p < 0.0001$ for both) with an AUC of 0.903 and 0.937, respectively (Fig. 4). Similarly, when patients were stratified based on amount of FGT, the difference between benign and malignant lesion ADC values was statistically significant among non-dense and dense breasts ($p = 0.0003$ and $p < 0.0001$, respectively) with an AUC of 0.887 and 0.924, respectively (Fig. 5). When stratified by menopausal status, differentiation of benign and malignant lesions was equally possible ($p < 0.0001$ for both) with an AUC of 0.938 in premenopausal and 0.892 in postmenopausal women (Fig. 6).

Discussion

Our findings show that DWI with ADC mapping distinguishes benign and malignant lesions with good sensitivity and specificity (87 % for both), and was not significantly influenced by the patient characteristics such as FGT, BPE and menopausal status. When patients were stratified according to BPE, FGT and menopausal status, there remained a significant difference in ADC values between benign and malignant lesions: malignant lesions consistently demonstrated significantly lower ADC values compared with benign lesions. Thus, our findings indicate that DWI with ADC mapping is equally accurate in breast cancer diagnosis regardless of different patient characteristics, and support its use as part of a standard imaging protocol for improved cancer diagnosis.

The role of DWI in breast imaging has been previously investigated, with several studies demonstrating that ADC is

Table 4 Comparison of ADC values between benign and malignant lesions stratified by background parenchymal enhancement (BPE), amount of fibroglandular tissue (FGT) and menopausal status

Variable	Benign lesions			Malignant lesions			<i>p</i> -value*
	N	ADC value (10 ⁻³ mm ² /s)		N	ADC value (10 ⁻³ mm ² /s)		
		Mean	SD		Mean	SD	
Overall lesions	130	1.529	0.262	218	1.072	0.213	<0.0001
Background parenchymal enhancement							
Low BPE	65	1.585	0.305	105	1.098	0.239	<0.0001
High BPE	65	1.472	0.199	113	1.048	0.190	<0.0001
Amount of fibroglandular tissue							
Non-dense breast	20	1.401	0.197	47	1.067	0.228	<0.0001
Dense breast	110	1.552	0.267	171	1.073	0.295	0.0003
Menopausal status							
Premenopausal	70	1.541	0.256	124	1.044	0.211	<0.0001
Postmenopausal	60	1.515	0.272	94	1.108	0.212	<0.0001

ADC apparent diffusion coefficient, BPE background parenchymal enhancement, FGT fibroglandular tissue, SD standard deviation

*Of comparison between benign and malignant lesions

a useful tool for characterizing breast lesions, even though optimal thresholds varied among these studies [9, 10, 15–19]. In a meta-analysis by Tsushima et al. [18], an ADC threshold value of 1.23×10^{-3} mm²/s for the differentiation of benign and malignant lesions was obtained with a pooled sensitivity and specificity of 89 % and 77 %, respectively. In our study, using a derived optimal threshold of 1.30×10^{-3} mm²/s, we achieved a sensitivity and specificity of 87 %, which is in good agreement with previously published reports [9, 10, 16, 17, 19].

To the best of our knowledge, this is the first study to investigate the impact of FGT, BPE as well as menopausal status on the diagnostic accuracy of DWI with ADC mapping for breast cancer diagnosis in one patient collective.

Several studies have had mixed findings for the effect of BPE on DWI ADC values, but none have evaluated the subsequent impact on diagnostic accuracy. When assessing the relationship of BPE and ADC of normal fibroglandular tissue, studies have shown conflicting results [22, 25, 27]. For example, in patients with normal breast DWI MRIs, McDonald et al. [27] found that whereas mammographic breast density and ADC of FGT are positively correlated, BPE and ADC of FGT are not. Similar correlations were observed by Iacconi et al. [25] in a population composed mainly of patients with breast cancer. Cho et al. [22] showed that patients with breast cancer exhibited significantly higher BPE values, but like the other studies BPE values were not correlated with ADC of FGT. On the other hand, different results were obtained by Kawamura et al. [26],

who found that BPE was inversely correlated with ADC of FGT. In our study, the sensitivity and specificity of DWI with ADC mapping in differentiating benign from malignant lesions was not statistically significantly affected by BPE.

In the current study, we employed a fat-suppressed sequence and did not observe a significant impact of amount of FGT on ADC values of both benign and malignant breast lesions. Previously, Partridge et al. assessed the influence of intravoxel fat signal on ADC values obtained using DWI with and without fat suppression for both tumour and normal FGT in a group of 21 women with diagnosed breast cancer [29]. In this study, there were systematic underestimations of ADCs for both tumour and normal breast tissue due to intravoxel contribution from fat signal on non-fat-suppressed DWI but not when adequate fat suppression was used. This was more pronounced for normal tissue than for tumours and was worse in women with mammographic low density than those with extremely dense breasts. These findings confirm the importance of a robust fat suppression for optimal diagnostic accuracy.

Studies that have investigated the impact of FGT or mammographic breast density on ADC values of healthy breast tissue in breast cancer patients or healthy volunteers have not yet evaluated its diagnostic accuracy for breast cancer diagnosis [22, 23, 25–27]. O'Flynn et al. [28], who investigated BRCA 1/2 mutation carriers and patients who had undergone supradiaphragmatic radiotherapy, showed that patients who had received radiation therapy to the breast had higher ADC values of FGT, which could improve the detection of

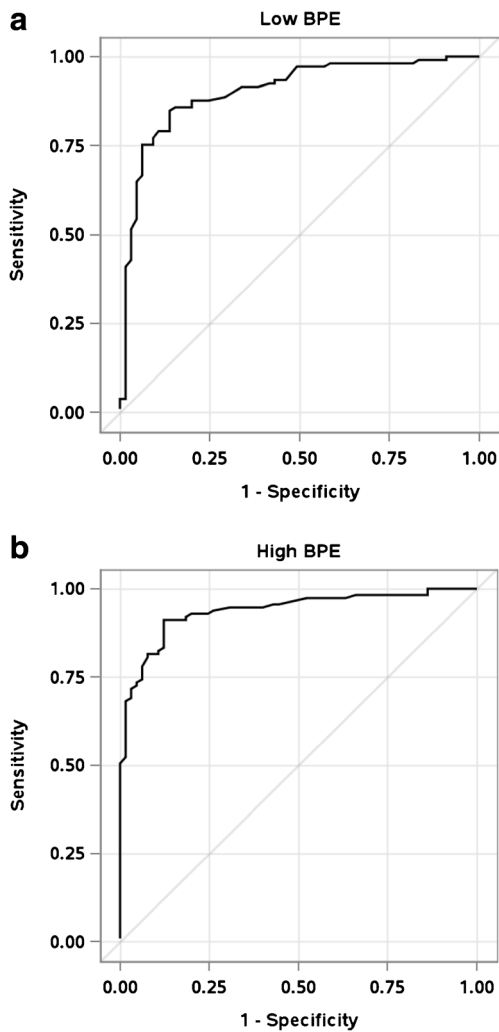


Fig. 4 Receiver operator characteristic (ROC) curve analysis of ADC values among low background parenchymal enhancement (BPE) (a) and high BPE (b) breasts for differentiation between benign and malignant lesions

malignant tumours. Fat necrosis induced by radiation therapy could be attributed to the higher ADC values found in that population. The FGT ADC also correlated with mammographic breast density in their study, being higher in dense breasts and lower in fatty ones. Even though the amount of fat in the breast may influence DWI, in our study the sensitivity and specificity of ADC in differentiating benign from malignant lesions were not statistically significantly different between dense and non-dense breasts.

Some studies have also evaluated the relationship between menstrual cycle and menopausal status with DWI [20, 21, 24]. A previous study by Clendenen et al. [24] demonstrated that the FGT ADC could be affected by the menstrual cycle. On the other hand, studies by El Khoully et al. [20] and Kim et al.

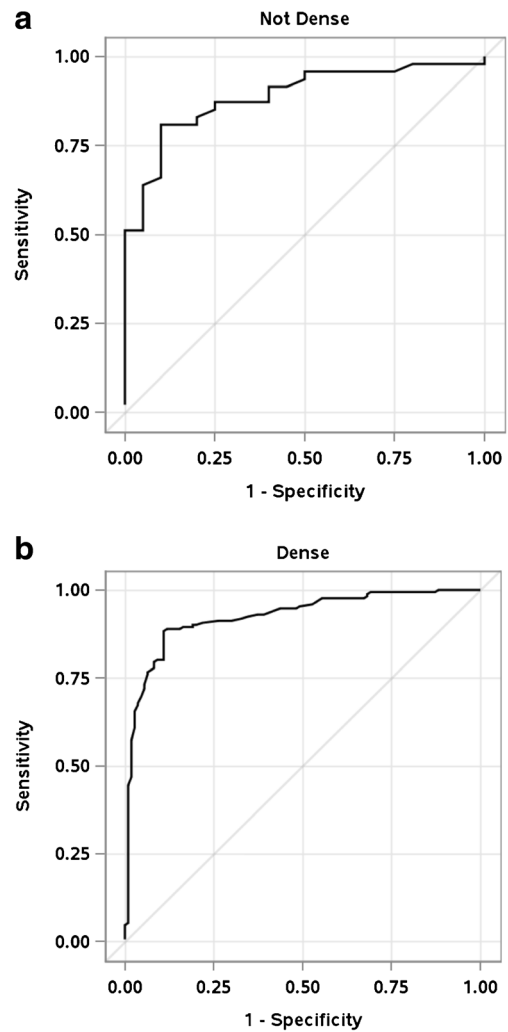


Fig. 5 Receiver operator characteristic (ROC) curve analysis of ADC values according to amount of FGT among non-dense (a) and dense (b) breasts for differentiation between benign and malignant lesions

[21], which evaluated the ADC values of benign and malignant lesions, did not find significant differences in the ADCs of premenopausal and postmenopausal women, similar to what was observed in our study. In our study, the accuracy for breast cancer diagnosis was not significantly different in pre- and postmenopausal patients.

Limitations

There were several limitations to our retrospective study. Due to the low spatial resolution of DWI, lesions smaller than 0.8 cm were not included. Therefore, insights into this specific subgroup are limited. Since the study was conducted in a comprehensive cancer centre, our population presented with a relatively high number of malignant compared to benign

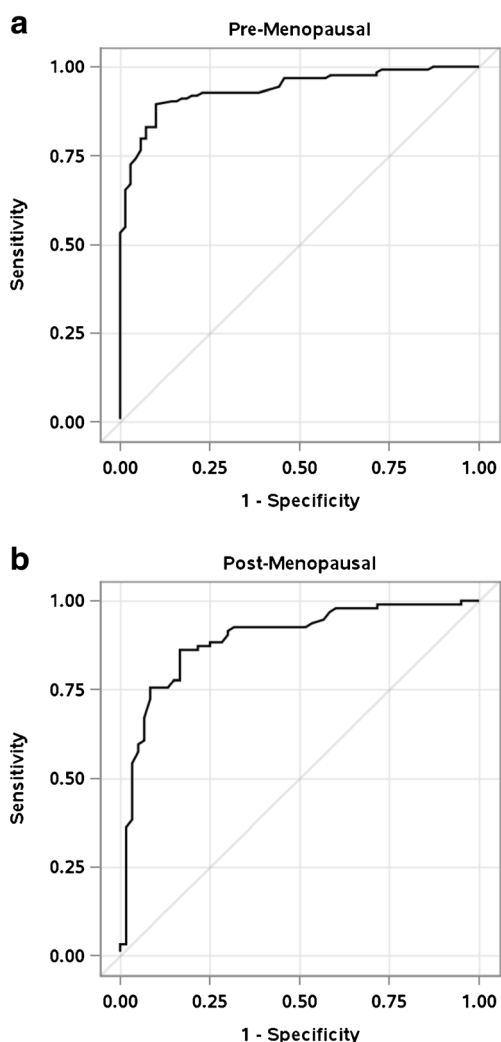


Fig. 6 Receiver operating characteristic (ROC) curve analysis of ADC values according to menopausal status among premenopausal (a) and postmenopausal (b) patients for differentiation between benign and malignant lesions

lesions. Additionally, a greater number of dense than non-dense breasts were found in our study population, which was composed mostly of premenopausal women under the age of 50 years.

Conclusion

In conclusion, our study demonstrated that DWI with ADC mapping enables the differentiation of benign from malignant lesions with high sensitivity and specificity. The diagnostic accuracy of DWI with ADC mapping is not significantly impacted by different levels of BPE, FGT and menopausal status. Therefore, data indicate that DWI with ADC can be added to a standard imaging protocol regardless of different patient characteristics for an improved breast cancer diagnosis.

Acknowledgements We would like to thank Joanne Chin for technical editing.

Funding This study has received funding by Memorial Sloan Kettering Cancer Center Support Grant / NIH Core Grant (P30 CA008748), DOD BCRP W81XWH-09-1-0042 grant, and the Breast Cancer Research Foundation grant of Memorial Sloan Kettering Cancer Center.

Compliance with ethical standards

Guarantor The scientific guarantor of this publication is Sunitha B. Thakur.

Conflict of interest The authors of this manuscript declare no relationships with any companies, whose products or services may be related to the subject matter of the article.

Statistics and biometry One of the authors has significant statistical expertise (Sujata Patil).

Informed consent Written informed consent was waived by the Institutional Review Board.

Ethical approval Institutional Review Board approval was obtained.

Study subjects or cohorts overlap Some study subjects or cohorts have been previously reported in Durando M, Gennaro L, Cho GY et al (2016) Quantitative apparent diffusion coefficient measurement obtained by 3.0Tesla MRI as a potential noninvasive marker of tumor aggressiveness in breast cancer. *Eur J Radiol* 85:1651-1658. However, different data were used in a different context.

Methodology

- retrospective
- observational
- performed at one institution

References

1. Mann RM, Balleyguier C, Baltzer PA et al (2015) Breast MRI: EUSOBI recommendations for women's information. *Eur Radiol* 25:3669–3678
2. Sardanelli F, Boetes C, Borisch B et al (2010) Magnetic resonance imaging of the breast: recommendations from the EUSOMA working group. *Eur J Cancer* 46:1296–1316
3. Kuhl CK, Strobel K, Bieling H, Leutner C, Schild HH, Schrading S (2017) Supplemental Breast MR Imaging Screening of Women with Average Risk of Breast Cancer. *Radiology* 283:361–370
4. Lehman CD, Smith RA (2009) The role of MRI in breast cancer screening. *J Natl Compr Canc Netw* 7:1109–1115
5. Lourenco AP, Donegan L, Khalil H, Mainiero MB (2014) Improving outcomes of screening breast MRI with practice evolution: initial clinical experience with 3T compared to 1.5T. *J Magn Reson Imaging* 39:535–539
6. Partridge SC, DeMartini WB, Kurland BF, Eby PR, White SW, Lehman CD (2009) Quantitative diffusion-weighted imaging as an adjunct to conventional breast MRI for improved positive predictive value. *AJR Am J Roentgenol* 193:1716–1722
7. Pinker K, Helbich TH, Morris EA (2017) The potential of multiparametric MRI of the breast. *Br J Radiol* 90:20160715

8. European Society of R (2010) White paper on imaging biomarkers. *Insights Imaging* 1:42–45
9. Tan SL, Rahmat K, Rozalli FI et al (2014) Differentiation between benign and malignant breast lesions using quantitative diffusion-weighted sequence on 3 T MRI. *Clin Radiol* 69:63–71
10. Guo Y, Cai YQ, Cai ZL et al (2002) Differentiation of clinically benign and malignant breast lesions using diffusion-weighted imaging. *J Magn Reson Imaging* 16: 172–178
11. White NS, McDonald CR, Farid N et al (2014) Diffusion-Weighted Imaging in Cancer: Physical Foundations and Applications of Restriction Spectrum Imaging. *Cancer Res* 74:4638–4652
12. Matsubayashi RN, Fujii T, Yasumori K, Muranaka T, Momosaki S (2010) Apparent diffusion coefficient in invasive ductal breast carcinoma: correlation with detailed histologic features and the enhancement ratio on dynamic contrast-enhanced MR images. *J Oncol* 2010:1–6. <https://www.hindawi.com/journals/jo/2010/821048/>
13. Martincich L, Deantoni V, Bertotto I et al (2012) Correlations between diffusion-weighted imaging and breast cancer biomarkers. *Eur Radiol* 22:1519–1528
14. Arlinghaus LR, Li X, Rahman AR et al (2011) On the relationship between the apparent diffusion coefficient and extravascular extracellular volume fraction in human breast cancer. *Magn Reson Imaging* 29:630–638
15. Partridge SC, Mullins CD, Kurland BF et al (2010) Apparent diffusion coefficient values for discriminating benign and malignant breast MRI lesions: effects of lesion type and size. *AJR Am J Roentgenol* 194:1664–1673
16. Caivano R, Villonio A, D' Antuono F et al (2015) Diffusion weighted imaging and apparent diffusion coefficient in 3 tesla magnetic resonance imaging of breast lesions. *Cancer Invest* 33:159–164
17. Suo S, Cheng F, Cao M et al (2017) Multiparametric diffusion-weighted imaging in breast lesions: Association with pathologic diagnosis and prognostic factors. *J Magn Reson Imaging* 46:740–750
18. Tsushima Y, Takahashi-Taketomi A, Endo K (2009) Magnetic resonance (MR) differential diagnosis of breast tumors using apparent diffusion coefficient (ADC) on 1.5-T. *J Magn Reson Imaging* 30: 249–255
19. Kul S, Eyuboglu I, Cansu A, Alhan E (2014) Diagnostic efficacy of the diffusion weighted imaging in the characterization of different types of breast lesions. *J Magn Reson Imaging* 40:1158–1164
20. Ei Khouli RH, Jacobs MA, Mezban SD et al (2010) Diffusion-weighted imaging improves the diagnostic accuracy of conventional 3.0-T breast MR imaging. *Radiology* 256:64–73
21. Kim JY, Suh HB, Kang HJ et al (2016) Apparent diffusion coefficient of breast cancer and normal fibroglandular tissue in diffusion-weighted imaging: the effects of menstrual cycle and menopausal status. *Breast Cancer Res Treat* 157:31–40
22. Cho GY, Moy L, Kim SG et al (2015) Comparison of contrast enhancement and diffusion-weighted magnetic resonance imaging in healthy and cancerous breast tissue. *Eur J Radiol* 84:1888–1893
23. Choi YJ, Chen JH, Yu HJ, Li Y, Su MY (2017) Impact of Different Analytic Approaches on the Analysis of the Breast Fibroglandular Tissue Using Diffusion Weighted Imaging. *Biomed Res Int* 2017: 1094354
24. Clendenen TV, Kim S, Moy L et al (2013) Magnetic resonance imaging (MRI) of hormone-induced breast changes in young premenopausal women. *Magn Reson Imaging* 31:1–9
25. Iacconi C, Thakur SB, Dershaw DD, Brooks J, Fry CW, Morris EA (2014) Impact of fibroglandular tissue and background parenchymal enhancement on diffusion weighted imaging of breast lesions. *Eur J Radiol* 83:2137–2143
26. Kawamura A, Satake H, Ishigaki S et al (2015) Prediction of background parenchymal enhancement on breast MRI using mammography, ultrasonography, and diffusion-weighted imaging. *Nagoya J Med Sci* 77:425–437
27. McDonald ES, Schopp JG, Peacock S et al (2014) Diffusion-weighted MRI: association between patient characteristics and apparent diffusion coefficients of normal breast fibroglandular tissue at 3 T. *AJR Am J Roentgenol* 202:W496–W502
28. O'Flynn EA, Wilson RM, Allen SD, Locke I, Scurr E, deSouza NM (2014) Diffusion-weighted imaging of the high-risk breast: Apparent diffusion coefficient values and their relationship to breast density. *J Magn Reson Imaging* 39:805–811
29. Partridge SC, Singer L, Sun R et al (2011) Diffusion-weighted MRI: influence of intravoxel fat signal and breast density on breast tumor conspicuity and apparent diffusion coefficient measurements. *Magn Reson Imaging* 29:1215–1221
30. Morris EA, Comstock CE, Lee CH, et al. (2013) ACR BI-RADS® magnetic resonance imaging. In: ACR BI-RADS® Atlas, Breast Imaging Reporting and Data System. American College of Radiology, Reston, VA
31. Youden WJ (1950) Index for rating diagnostic tests. *Cancer* 3:32–35